

Circ_KIAA0922 regulates Saos-2 cell proliferation and osteogenic differentiation by regulating the miR-148a-3p/SMAD5 axis and activating the TGF- β signaling pathway

Shanshan Zhang, Yongtao Zhang, Dan Yang, Wei Zhi, Junfeng Li, Meilin Liu, Yanqin Lu*, Jinxiang Han*

Key Laboratory for Biotech-Drugs of National Health Commission, Key Laboratory for Rare & Uncommon Diseases of Shandong Province, Biomedical Sciences College & Shandong Medicinal Biotechnology Centre, Shandong First Medical University & Shandong Academy of Medical Sciences, Ji'nan, Shandong, China.

SUMMARY Circular RNAs (circRNAs) are emerging as important regulators in human disease, but their function in osteoporosis (OP) is not sufficiently known. The aim of this study was to identify the possible molecular mechanism of circ_KIAA0922 in osteogenic differentiation of Saos-2 cells *in vitro* and the interactions among circ_KIAA0922, miR-148a-3p, and SMAD family member 5 (SMAD5). Circ_KIAA0922, miR-148a-3p, and SMAD5 were overexpressed by transient transfection. Dual-luciferase reporter assay system was used to analyze the combination among circ_KIAA0922, miR-148a-3p, and SMAD5. In addition, the levels of circ_KIAA0922, miR-148a-3p, SMAD5, osteocalcin (OCN), and runt-related transcription factor 2 (RUNX2) were detected using RT-qPCR or western blot analysis. Alizarin red staining was performed to analyze the degree of osteogenic differentiation under the control of circ_KIAA0922, miR-148a-3p, and SMAD5. We found that circ_KIAA0922 knockdown inhibited the proliferation and osteogenic differentiation of Saos-2 cells. Circ_KIAA0922 directly targeted miR-148a-3p, and miR-148a-3p inhibition reversed the effects of circ_KIAA0922 knockdown on the proliferation and osteogenic differentiation of Saos-2 cells. Overexpression of SMAD5 promoted the proliferation and osteogenic differentiation of Saos-2 cells and attenuated the inhibitory effect of miR-148a-3p on cell proliferation and osteogenic differentiation. In conclusion, circ_KIAA0922 facilitated Saos-2 cell proliferation and osteogenic differentiation *via* the circ_KIAA0922/miR-148a-3p/SMAD5 axes *in vitro*, thus providing insights into the mechanism of osteogenic differentiation by circ_KIAA0922.

Keywords Circ_KIAA0922, miR-148a-3p, SMAD5, cell proliferation, osteogenic differentiation

1. Introduction

Bone homeostasis is a dynamic balance between bone formation by osteoblasts and bone resorption by osteoclasts (1). In case of an imbalance, various destructive bone diseases such as OP occur (2). OP is a debilitating bone disease with a high prevalence worldwide and is the most common in older individuals, especially in postmenopausal women (3). Because the incidence of osteoporotic fractures increases with advancing age, measures to diagnose and prevent OP and its complications are of major public health importance (4,5). There is accumulating evidence that epigenetic modifications may be mechanisms underlying the links of genetic and environmental factors with increased risk of OP and bone fracture. It has been shown that

some forms of RNAs, such as microRNAs (miRNAs), long noncoding RNAs (lncRNAs), and circular RNAs (circRNAs), are epigenetic regulators with significant involvement in the control of gene expression, and as such they affect multiple biological processes, including bone metabolism.

CircRNAs are a new type of noncoding RNAs with a closed continuous loop structure formed by covalent concatenating of the 3'-poly(A) tails and 5'-end capping splice sites. They were first found in viroid in 1976, but are widely distributed in nature (6). Previous studies have demonstrated that some circRNAs have a function of microRNA "sponges", which can offset microRNA-mediated mRNA inhibition (7), thereby participating in epigenetic regulation and transcriptional and posttranscriptional regulation by different mechanisms

(8). There is substantial evidence that circRNAs have a major role in the development of OP, and their great potential as biomarkers and therapeutic targets for OP is being elucidated (9,10). It has been shown that circRNAs are differentially expressed in postmenopausal OP. Target prediction and dual luciferase reporter gene assay have shown that circ_0016624 sponge inhibits miR-98 and circ_0048211 sponge inhibits miRNA-93-5p, which increases BMP-2 expression and promotes the transformation of stem cells into osteoblasts (11,12). According to Yao *et al.*, senile OP is associated with the regulation of circRNA expression (13,14). Next-generation sequencing and RT-qPCR have revealed that circ_KIAA0922 is downregulated in a murine asthma model group compared with the control group (15). Xie *et al.* have reported that the downregulation of 28 annotated circRNAs, including circ_KIAA0922, characterizes high-cholesterol diet-induced nonalcoholic fatty liver disease (16). However, there have not yet been reports on the role of circ_KIAA0922 in bone differentiation.

MicroRNAs (miRNAs) are a type of noncoding RNAs with a regulatory function and a length of approximately 20–25 nucleotides, which identify target mRNAs according to the principle of complementary base pairing and guide the silencing complex to degrade the target mRNAs or repress the translation of mRNAs (17). In addition to circRNAs, osteoclast differentiation involves dysregulation and function of miRNAs, such as miR-7223-5p (18), miR-19b (19), and miR-125b (20). Liu *et al.* have demonstrated the inhibitory effect of miR-148a-3p on osteoblast differentiation and bone remodeling (21). However, it remains unknown whether miR-148a-3p mediates the function of circ_KIAA0922 in OP.

SMAD5 is an intracellular signal transducer for the transforming growth factor- β (TGF- β) superfamily, which is classified into TGF- β s, activins, and bone morphogenetic proteins (BMPs). As one of the receptor-activated Smad molecules (R-Smad), Smad5 is directly phosphorylated by activated type I TGF- β receptors and associates with the common Smad, Smad4, to form a heteromeric complex, which moves to the nucleus to act as a transcription factor. Many studies have demonstrated that bone morphogenetic proteins (BMPs) and TGF- β are the most important cytokines affecting the differentiation of osteoblasts. BMP-2 is a member of the TGF- β superfamily that is a key signaling component in osteoblast differentiation. Smad5 is a downstream transcription factor that is phosphorylated and activated by BMP-2 receptors. SMAD5 is an important element involved in the TGF- β signaling pathway. Activated SMAD5 stimulates the TGF- β signaling pathway. According to Wang *et al.*, miR-148a and SMAD5 participate in the regulation of pancreatic stellate cell activation through a mechanism that involves competing endogenous RNA (17).

In the present study, SMAD5 was considered the candidate target gene regulated by miRNA-148a-3p. The role of circ_KIAA0922 in osteogenic differentiation of Saos-2 cells *via* the miRNA-148a-3p/SMAD5/TGF- β axis is also worth further investigation. Taken together, our study aimed to investigate the effects of circ_KIAA0922 on the proliferation and osteogenic differentiation of cultured Saos-2 cells and to clarify its regulatory effects on miR-148a-3p.

2. Materials and Methods

2.1. Cell culture and osteogenic induction

The human osteosarcoma cell line (Saos-2 cells) was purchased from the cell bank of the Chinese Academy of Science (Shanghai, China). Saos-2 cells were cultured in McCoy's 5A medium (Gibco, Rockville, MD, USA) supplemented with 10% fetal bovine serum (FBS; Gibco, Rockville, MD, USA) and 1% penicillin–streptomycin (Beyotime Biotechnology, Shanghai, China) at 37°C in an atmosphere containing 5% CO₂. The culture medium was changed every two days. For subcultures, the cells at 80–90% confluence were passaged at a ratio of 1:2 using 0.25% trypsin (Beyotime Biotechnology, Shanghai, China). When the cells again grew to 80–90% confluence, they were exposed to McCoy's 5A complete medium containing 2% FBS. The cells were subjected to cell proliferation assay and transfection.

When Saos-2 cells reached 80% confluence, they were cultured in osteoblast medium (OM) supplemented with 10% FBS, 200 μ M L-ascorbic acid (Sangon, Shanghai, China), 10 mM glycerophosphate (Sigma-Aldrich, St. Louis, MO, USA), and 100 nM dexamethasone (Sangon) to induce osteoblastic differentiation. The osteogenic induction medium was changed every 3 days, and the cells were collected after 0, 3, 7, and 14 days of differentiation. Saos-2 cells cultured in the growth medium (GM) were used as controls.

2.2. Cell transfection

Small interfering RNA (siRNA) against circ_KIAA0922 (si-circ_KIAA0922) or circ_KIAA0922 overexpression vector (circ_KIAA0922) was synthesized to knock down or elevate circ_KIAA0922 expression, respectively, with si-NC or pCD2.1-ciR utilized as control. The mimic or inhibitor of miR-148a-3p (miR-148a-3p or anti-miR-148a-3p) was used to increase or decrease miR-148a-3p expression, respectively, while miR-NC or anti-miR-NC was used as scramble control. Moreover, siRNA targeting SMAD5 or SMAD5 overexpression was employed to reduce or enhance SMAD5 expression, respectively, while si-control or pcDNA was used as control. All of the above vectors or oligonucleotides were synthesized by GenePharma Co., Ltd. (Shanghai, China). Cell transfection was executed using Lipofectamine 2000

(Invitrogen, Carlsbad, CA, USA) in accordance with the described protocols.

2.3. Cell counting kit-8

Cell counting kit-8 (CCK-8; Beyotime Biotechnology, Shanghai, China) assay was performed to determine the viability of Saos-2 cells. A total of 2×10^3 cells were seeded into 96-well cell culture plates and maintained at 37°C. At each of the desired time points, the plates were cultured for 4 h after adding 10 µL CCK-8 reagent to each well. Next, the wavelength at 450 nm was determined using a microplate reader (Bio-Rad Laboratories, Richmond, CA, USA).

2.4. Quantitative real-time polymerase chain reaction (qRT-PCR)

Total RNA from Saos-2 cells was extracted by TRIzol RNA reagent (Invitrogen, Carlsbad, CA, USA), and 1 µg of RNA sample was prepared for reverse transcription into cDNA using PrimeScriptRT kit (TaKaRa, Shiga, Japan). With cDNA as the template, the noncoding RNA and gene expression levels were analyzed by PCR using SYBR qPCR Master Mix (Sparkjade, Jinan, China) on the Applied Biosystems 7500 Real-time Fast PCR System. By using the $2^{-\Delta\Delta Ct}$ method, the expression was computed with GAPDH or U6 as the internal control. The primers used are presented in Table 1.

2.5. RNase R treatment

To estimate the stability of circ_KIAA0922, the RNA in Saos-2 cells was treated with or without (Mock) RNase R (Epicenter Biotechnologies, Madison, WI, USA) at 37°C for 30 min. Following RNase R treatment, qRT-PCR was performed to detect the expression levels of circ_KIAA0922 and GAPDH.

2.6. Isolation of nuclear and cytoplasmic fractions

In brief, 1×10^6 cultured Saos-2 cells were rinsed in phosphate-buffered saline (PBS) and placed into the cell fractionation buffer and cell disruption buffer in sequence. The fractions of cell cytoplasm or cell nucleus were individually separated in line with the manual of PARIS™ kit (Invitrogen). The expression levels of circ_KIAA0922, U6, and GAPDH were analyzed by qRT-PCR.

2.7. Western blot assay

Total protein in Saos-2 cells was isolated by RIPA lysis buffer (Beyotime Biotechnology, Shanghai, China) and quantified utilizing a BCA protein quantification kit (Vazyme, Nanjing, China). Then, the proteins were separated by 10% SDS-PAGE electrophoresis and subsequently transferred onto PVDF membranes (Invitrogen, Carlsbad, CA). The membranes were blocked with 5% defatted milk for 1 h and incubated with primary antibodies against runt-related transcription factor 2 (RUNX2) (bs-1134R; 1:2000; Bioss, Beijing, China), osteocalcin (OCN) (bs-4917R; 1:2000; Bioss), SMAD5 (ab40771; 1:20000; Abcam), transforming growth factor beta 1 (TGFβ1) (bs-0086R; 1:1500; Bioss), transforming growth factor beta 2 (TGFβ2) (bs-20412R; 1:1500; Bioss), bone morphogenetic protein 4 (BMP4) (bs-1374R; 1:2000; Bioss) and GAPDH (ab9485; 1:10000; Abcam) at 4°C overnight. After that, the membranes were probed with horseradish peroxidase-conjugated secondary antibody (bs-40296G-HRP; 1:10,000; Bioss) for 1 h at room temperature. The protein bands were visualized *via* ECL kit (Vazyme, Nanjing, China) and quantified using ImageJ software.

2.8. Alizarin Red-S (ARS) staining assay

To detect calcium deposition in the extracellular matrix, Saos-2 cells were subjected to 3, 7, and 14 days of incubation in the osteogenic medium in 24-well plates. After fixation, calcified nodules were treated with 0.1% Alizarin red S solution (Beyo time, Shanghai, China) at pH 4.2. Images were obtained using a microscope (Olympus, Japan). Cetylpyridine chloride (CPC, 100 mM) was used to dissolve calcified nodules, and the relative calcium mass was calculated based on the absorbance at 562 nm.

2.9. Dual-luciferase reporter assay

We used online bioinformatics software (circBank and StarBase) to predict the targets of circ_KIAA0922 and miR-148a-3p. The results showed that miR-148a-3p could potentially be targeted by circ_KIAA0922 and that SMAD5 was a larvaceous target of miR-148a-3p. The circ_KIAA0922 or SMAD5 3'UTR fragment containing the wild-type (WT) or mutant-type (MUT) binding site of miR-148a-3p was cloned into pmirGLO (Geneseeed,

Table 1. Primers sequences used for qRT-PCR

Name of primer	Sequences (5'-3')
hsa-circ-KIAA0922	Forward ACAAAGCCTTCTTCAGAAAAGA
	Reverse GTGCTTGTTGGAAGGCTATTA
OCN	Forward CTGACCTCACAGATGCCAAGC
	Reverse TGGTCTGATAGCTCGTCACAAG
RUNX2	Forward AGCAAGGTTCAACGATCTGAGAT
	Reverse TTTGTGAAGACGGTTATGGTCAA
hsa-miR-148a-3p	Forward TCAGTGCCTACAGAACTTTGT
	Reverse GAATACCTCGGACCCTGC
SMAD5	Forward CCAGCAGTAAAGCGATTGTTGG
	Reverse GGGGTAAGCCTTTTCTGTGAG
U6	Forward GCTTCGGCAGCACATATACTAA
	Reverse AACGCTTCACGAATTTGCGT
hsa-GAPDH	Forward GGTGTTTCAGCACCTCTACC
	Reverse TGTAGCACTTGGCTTTGGAG

Guangzhou, China) to obtain circ_KIAA0922, MUT-circ_KIAA0922, WT-SMAD5 3'UTR, and MUT-SMAD5 3'UTR. The generated vector was cotransfected with miR-148a-3p/miR-NC into Saos-2 cells. At length, a Dual-Luciferase Reporter Assay System (Vazyme, Nanjing, China) was prepared for detecting luciferase vectors at 48 h after transfection. At least three biological replicates were performed to compare luciferase activity between the groups.

2.10. RNA immunoprecipitation assay

The EZMagna RIP-Kit (Millipore Burlington, MA, USA) was used in accordance with the protocols. Target cells were lysed in a complete RNA immunoprecipitation (RIP) lysis buffer, and the cell extract was incubated with magnetic beads conjugated with anti-Argonaute 2 (AGO2) or control anti-IgG antibody (Millipore) for 6 h at 4°C, followed by incubation with Proteinase K to remove the proteins. Purified RNA was analyzed using real-time PCR. Next, enrichment analysis of circ_KIAA0922, miR-148a-3p, and SMAD5 was performed.

2.11. RNA pull-down assay

Magnetic beads (Thermo Fisher Scientific, Waltham, MA) were incubated with a biotin-labeled miR-148a-3p probe (bio-miR-148a-3p; RiboBio, Guangzhou, China) and a bio-negative control probe (bio-miR-NC; RiboBio) at 4°C overnight. Saos-2 cells were lysed, and the cell lysates were collected and incubated with magnetic beads. Then, the magnetic beads were purified, and the enrichment of circ-KIAA922 and SMAD5 in bio-miR-

148a-3p and bio-miR-NC was detected using qRT-PCR.

2.12. Statistical analysis

The results are presented as the mean \pm standard error of the mean (SEM). Statistical comparisons were made with one-way ANOVA and the Tukey multiple-comparison tests using GraphPad Prism software, version 7.0 (GraphPad Software Inc., San Diego, CA, USA) to identify significant differences. *P* values lower than 0.05 were considered statistically significant (* represents $P < 0.05$, ** represents $P < 0.01$, *** represents $P < 0.001$). All experiments were performed at least three times.

3. Results

3.1. Characterization and expression analysis of circ_KIAA0922

Circ_KIAA0922 (chr4: 154524454–154533552), located on chromosome 4, is derived from exon 24 to exon 26 (928 bp) of the host gene KIAA0922 *via* back-splicing. By designing divergent primers and Sanger sequencing, we confirmed the predicted junction of circ_KIAA0922 (Figure 1A). To verify the characterization of circ_KIAA0922, we first designed specific primers to amplify linear and circ_KIAA0922 sequences. qRT-PCR analysis suggested that circ_KIAA0922 amplification product was only observed in cDNA by divergent primers but not in gDNA (Figure 1B). Then, Oligo (dT)18 primers reverse-transcript cDNA could barely amplify circ_KIAA0922 compared with Random primers (Figure 1C). In addition, RNase R assay showed that circ_KIAA0922

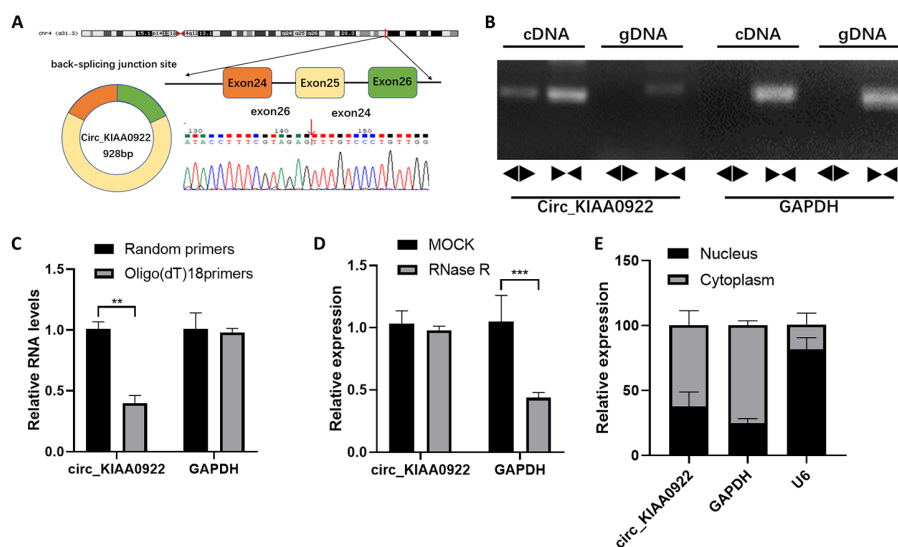


Figure 1. Characterization and expression analysis of circ_KIAA0922. (A) Schematic illustration of the genomic location and back splicing of circ_KIAA0922 with the splicing site validated by Sanger sequencing. (B) RT-PCR with divergent and convergent primers and agarose gel electrophoresis analysis were performed to detect the presence of circ_KIAA0922 and its maternal gene KIAA0922 in cDNA and gDNA samples from Saos2 cells. (C) The RNA in Saos-2 cells was reversely transcribed using Oligo (dT)18 primers or Random primers, and the expression of circ_KIAA0922 and GAPDH was detected. (D) RNase R treatment was used to evaluate the stability of circ_KIAA0922 and GAPDH mRNA in Saos-2 cells. (E) The expression of circ_KIAA0922 in the nucleus and cytoplasm of Saos-2 cells was examined with qRT-PCR.

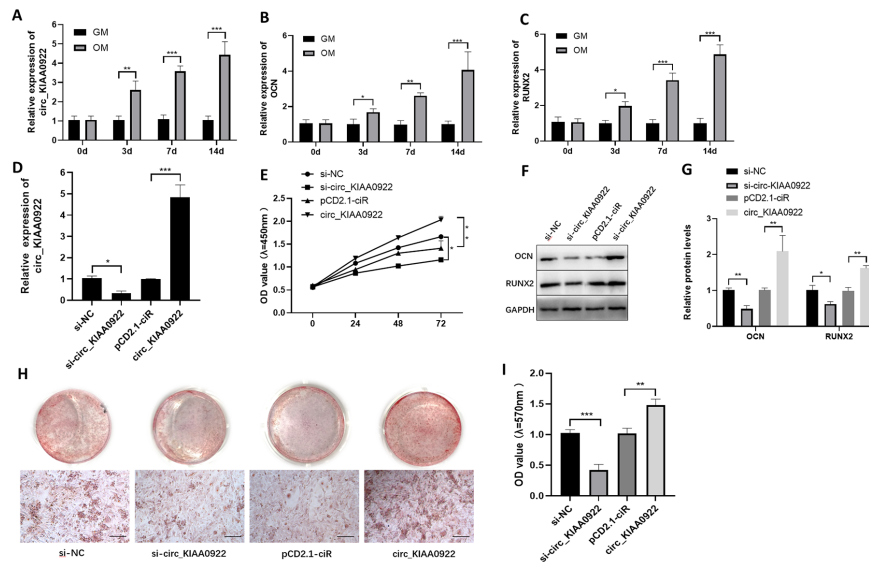


Figure 2. Circ_KIAA0922 contributes to the process of osteogenic differentiation of Saos-2 cells *in vitro*. (A-C) The expression of circ_KIAA0922, OCN and RUNX2 in GM- or OM-treated Saos-2 cells was detected by qRT-PCR. (D-I) Saos-2 cells were transfected with si-NC, si-circ_KIAA0922, pCD2.1-ciR, or circ_KIAA0922. (D) The expression of circ_KIAA0922 in transfected Saos-2 cells was detected by qRT-PCR. (E) The proliferation of Saos-2 cells was assessed by CCK-8 assay. (F and G) The protein levels of OCN and RUNX2 in Saos-2 cells were measured *via* western blot. (H and I) Alizarin Red staining was used to analyze the calcification of osteogenic differentiation.

was resistant to RNase R treatment, while GAPDH was evidently digested by RNase R (Figure 1D). Subcellular fraction analysis indicated that circ_KIAA0922 was mainly located in the cytoplasm rather than in the nucleus of Saos-2 cells (Figure 1E). These findings indicate that circ_KIAA0922 possesses a ring structure and that it is stable.

3.2. Circ_KIAA0922 contributes to the process of osteogenic differentiation of Saos-2 cells *in vitro*

To explore the role of circ_KIAA0922 in the osteogenic differentiation of Saos-2 cells, Saos-2 cells were induced with OM for indicated times, with GM-treated groups used as controls, and transfected with si-circ_KIAA0922 or circ_KIAA0922 overexpression vector to silence or potentiate circ_KIAA0922 expression, respectively. We found that circ_KIAA0922 level after osteogenic induction was markedly increased relative to that in the GM groups (Figure 2A). Next, we detected the expression of the osteogenesis-related markers OCN and RUNX2 in Saos-2 cells treated with GM or OM for 0, 3, 7, and 14 days. We found that OCN and RUNX2 levels were enhanced in OM-induced Saos-2 cells compared with GM-treated Saos-2 cells (Figure 2B-C). All these findings indicated that circ_KIAA0922 might be related to the progression of OP. In addition, si-circ_KIAA0922 transfection markedly suppressed circ_KIAA0922 expression, and circ_KIAA0922 overexpression vector transfection evidently enhanced circ_KIAA0922 expression in Saos-2 cells compared with si-NC or pCD2.1-ciR control groups (Figure 2D). Next, CCK-8 assay was performed to explore the effect of circ_KIAA0922 on the proliferation of Saos-2 cells after 3 days of OM induction. The results showed that circ_KIAA0922 knockdown repressed the proliferation of Saos-2 cells, whereas circ_KIAA0922 overexpression promoted the proliferation of Saos-2 cells (Figure 2E).

The results of western blot assay showed that silencing of circ_KIAA0922 decreased the protein levels of OCN and RUNX2 in Saos-2 cells after 3 days of OM induction, while overexpression of circ_KIAA0922 increased OCN and RUNX2 levels (Figure 2F-G). Alizarin Red staining revealed that the matrix mineralization level was decreased by silencing circ_KIAA0922 and increased by elevating circ_KIAA0922 (Figure 2H-I). The elevated OCN level, RUNX2 level, and matrix mineralization level demonstrated the promotional effect of circ_KIAA0922 on osteogenic differentiation of Saos-2 cells *in vitro*.

3.3. Circ_KIAA0922 acts as the sponge for miR-148a-3p

To explore the potential target miRNAs of circ_KIAA0922, the online prediction websites starBase 2.0, circBank and RegRNA 2.0 were used. As displayed in Venn diagram, seven candidate miRNAs (miR-34a-5p, miR-130a-3p, miR-130b-3p, miR-148a-3p, miR-152-3p and miR-145-5p) were found to contain the putative binding sites on circ_KIAA0922 (Figure S1, <http://www.irdrjournal.com/action/getSupplementalData.php?ID=174>). The effect of overexpression or knockdown of circ_KIAA0922 on the expression of the aforementioned miRNA in Saos-2 cells was detected by qRT PCR. The results showed that overexpression of circ_KIAA0922 significantly inhibited the expression of miR-148a-3p and 148b-3p in Saos-2 cells, with the most significant inhibitory effect on miR-148a-3p (Figure S2A, <http://www.irdrjournal.com/action/getSupplementalData.php?ID=174>). In Saos-2 cells, knocking down circ_KIAA0922 significantly promoted the expression of miR-148a-3p and miR-148b-3p. However, the promotion effect on miR-148a-3p is the most significant (Figure S2B, <http://www.irdrjournal.com/action/getSupplementalData.php?ID=174>). Therefore, it is speculated that the circ_KIAA0922

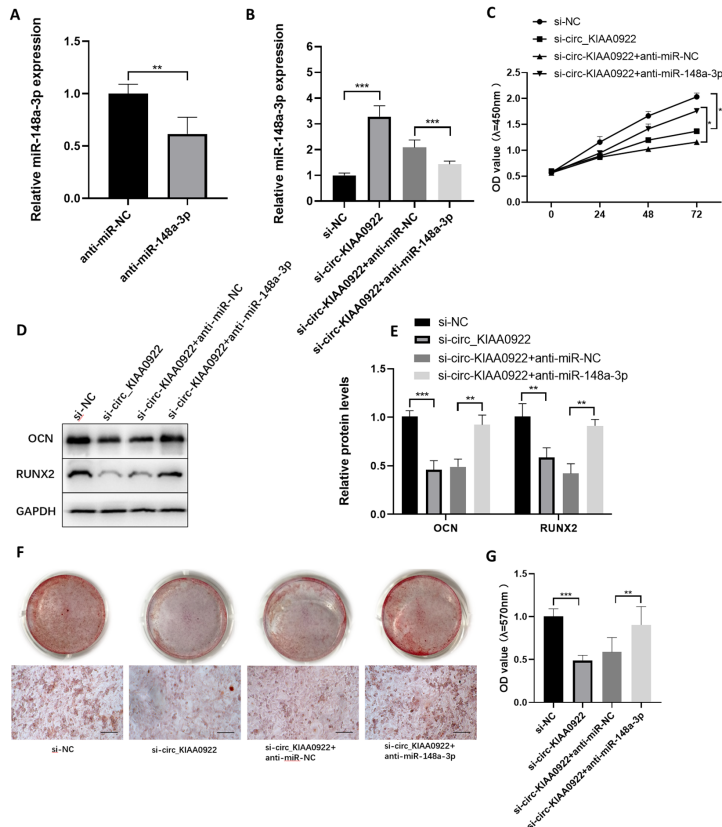


Figure 4. Circ_KIAA0922 silencing inhibits osteogenic differentiation of Saos-2 cells by targeting miR-148a-3p. (A) The expression of miR-148a-3p in Saos-2 cells transfected with anti-miR-NC or anti-miR-148a-3p was detected by qRT-PCR. (B-E) Saos-2 cells were transfected with si-NC, si-circ_KIAA0922, si-circ_KIAA0922 + anti-miR-NC, or si-circ_KIAA0922 + anti-miR-148a-3p. (B) MiR-148a-3p expression in Saos-2 cells was determined by qRT-PCR. (C) The proliferation of Saos-2 cells was evaluated by CCK-8 assay. (D and E) The protein levels of OCN and RUNX2 in Saos-2 cells were measured by western blot assay. (F and G) Alizarin Red staining assays were used to determine the ability of osteogenic differentiation of Saos-2 cells. Scale bar, 100 μ m.

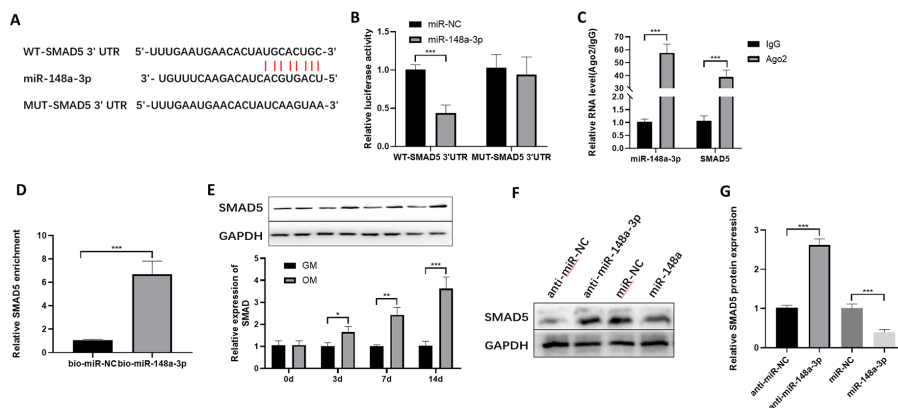


Figure 5. SMAD5 was targeted by miR-148a-3p. (A) The binding sites between SMAD5 and miR-148a-3p were exhibited. (B-D) The relationship between miR-148a-3p and SMAD5 was analyzed by dual-luciferase reporter assay, RIP assay, and RNA pull-down assay. (E) The protein level of SMAD5 in Saos-2 cells treated with OM or GM was measured by western blot assay. (F and G) The protein level of SMAD5 in Saos-2 cells transfected with anti-miR-NC, anti-miR-148a-3p, miR NC, or miR-148a-3p was measured by western blot.

5C). The results of RNA pull-down assay suggested that the enrichment of SMAD5 was promoted by bio-miR-148a-3p (Figure 5D). Moreover, SMAD5 protein level was increased in Saos-2 cells after OM induction (Figure 5E). In addition, anti-miR-148a-3p transfection elevated SMAD5 protein level, whereas miR-148a-3p mimic transfection reduced SMAD5 protein level in Saos-2 cells (Figure 5F-G). All these findings suggest that miR-148a-3p interacts with SMAD5 and negatively regulates SMAD5 expression.

3.6. SMAD5 promotes the osteogenic differentiation of Saos-2 cells

To explore the roles of SMAD5 in osteogenic differentiation in Saos-2 cells, Saos-2 cells were transfected with si-SMAD5 or SMAD5. The results of western blot assay showed that si-SMAD5 transfection decreased SMAD5 expression, whereas SMAD5 transfection increased SMAD5 expression compared with relevant controls (Figure 6A-B). The results of CCK-8 assay indicated that SMAD5 knockdown inhibited Saos-2 cells proliferation, whereas SMAD5 overexpression promoted Saos-2 cells proliferation (Figure 6C). Silencing of SMAD5 reduced the protein levels of OCN and RUNX2 in Saos-2 cells, while overexpression of SMAD5 led to the opposite

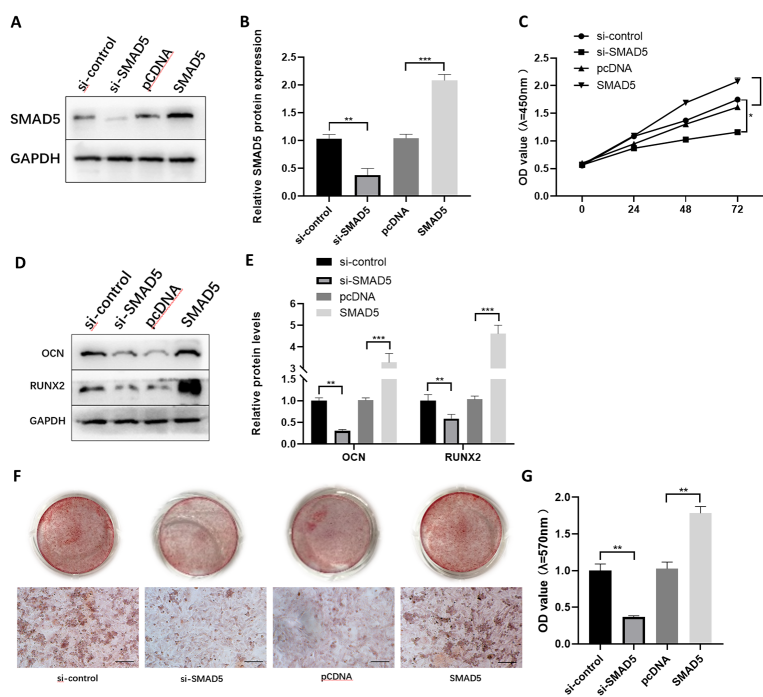


Figure 6. SMAD5 promotes the osteogenic differentiation of Saos-2 cells. Saos-2 cells were transfected with si-control, si-SMAD5, pcDNA, or SMAD5. (A and B) The protein level of SMAD5 in Saos-2 cells was measured via western blot. (C) The proliferation of Saos-2 cells was assessed by CCK-8 assay. (D and E) The protein levels of OCN and RUNX2 in Saos-2 cells were measured by western blot. (F and G) The osteogenic differentiation of Saos-2 cells was examined by Alizarin Red staining.

results (Figure 6D-E). As suggested by Alizarin Red staining, SMAD5 knockdown repressed osteogenic differentiation of Saos-2 cells, while SMAD5 overexpression promoted osteogenic differentiation of Saos-2 cells (Figure 6F-G). In summary, SMAD5 overexpression promotes osteogenic differentiation of Saos-2 cells *in vitro*.

3.7. MiR-148a-3p directly targets SMAD5 to regulate osteogenic differentiation of Saos-2 cells

As shown in Figure 7A-B, miR-148a-3p mimic transfection inhibited SMAD5 protein level in Saos-2 cells, but the effect was rescued by the introduction of the SMAD5 overexpression vector. CCK-8 assay indicated that the proliferation of Saos-2 cells was repressed by miR-148a-3p overexpression, but the effect was weakened by elevating SMAD5 (Figure 7C). Overexpression of miR-148a-3p decreased the protein levels of OCN and RUNX2 in Saos-2 cells, whereas SMAD5 upregulation abrogated these effects (Figure 7D-E). Moreover, based on Alizarin Red staining, miR-148a-3p overexpression suppressed osteogenic differentiation of Saos-2 cells, whereas SMAD5 enhancement moderated the effect (Figure 7F-G). Circ_KIAA0922 knockdown reduced the mRNA and protein levels of SMAD5 in Saos-2 cells, while miR-148a-3p inhibition reversed these effects (Figure 7H-G). All these findings suggest that SMAD5 overexpression weakens miR-148a-3p overexpression-mediated inhibition of osteogenic differentiation of Saos-2 cells *in vitro*.

3.8. circ_KIAA0922 targets miR-148a-3p/SMAD5 to

regulate osteogenic differentiation and activates the TGF- β signaling pathway in Saos-2 cells

As shown in Figure 8A-B, the proteins involved in the TGF- β signaling pathway, namely, TGF- β 1, TGF- β 2, and BMP4, were downregulated after miR-148a-3p overexpression, but upregulated after miR-148a-3p downregulation in Saos-2 cells. The promotive effect of miR-148a-3p overexpression on the protein expression levels was rescued by simultaneously overexpressing SMAD5 or circ_KIAA0922. Therefore, the TGF- β signaling pathway in Saos-2 cells was activated by the upregulation of circ_KIAA0922, which resulted in the downregulation of miR-148a-3p and the overexpression of SMAD5. The RNA-induced silencing complex (RISC) led by miR-148a-3p degraded SMAD5 mRNA, while circ_KIAA0922 bound miR-148a-3p to reduce the degradation of SMAD5 (Figure 8C). circ_KIAA0922 upregulated SMAD5 and TGF- β signaling pathway in Saos-2 cells through targeting miR-148a-3p, thereby influencing the progression of osteogenic differentiation of Saos-2 cells.

4. Discussion

OP is a bone metabolic disorder characterized by decreased bone density and deteriorated microstructure, which increases the risk of fractures. The imbalance between bone formation and bone resorption results in the occurrence and progression of OP. Bone homeostasis in the human body is a dynamic equilibrium that consists of bone formation and bone resorption processes. Imbalance and dysfunction of bone homeostasis are the basis of many skeletal diseases, including OP (Kim

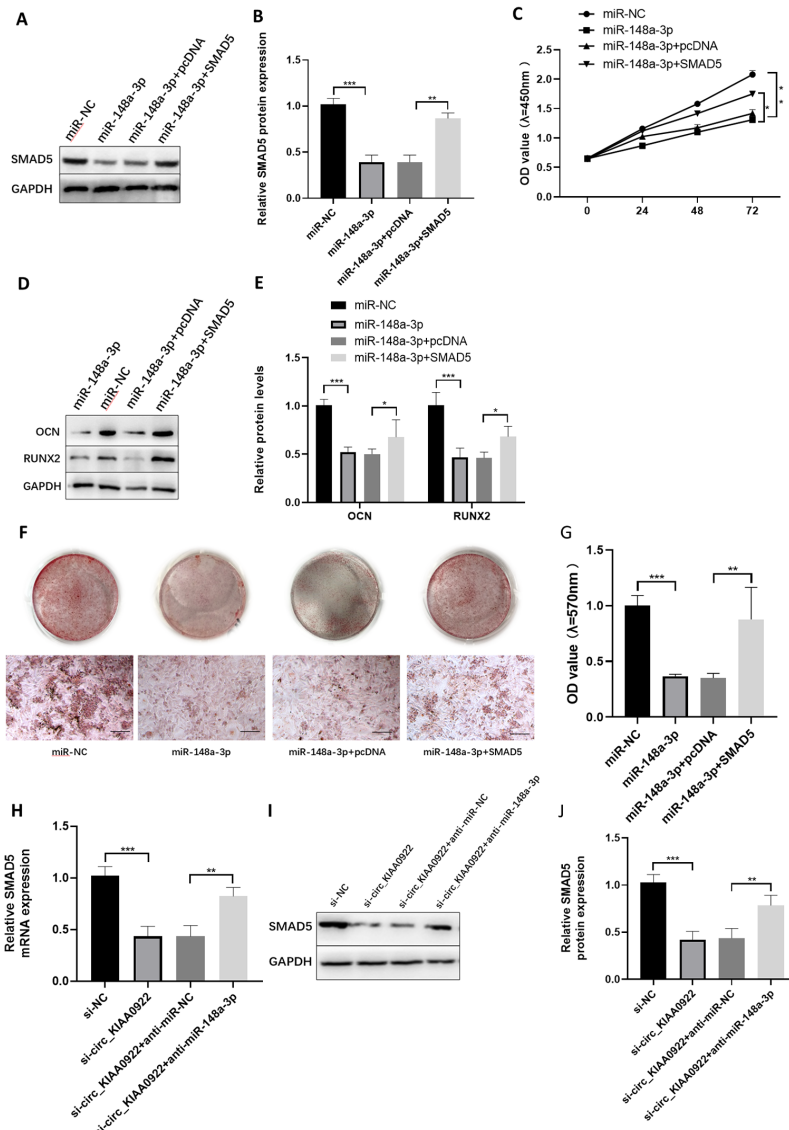


Figure 7. MiR-148a-3p directly targets SMAD5 to regulate osteogenic differentiation of Saos-2 cells. (A-D) Saos-2 cells were transfected with miR-NC, miR-148a-3p, miR-148a-3p + pcDNA or miR-148a-3p + SMAD5. (A and B) The protein level of SMAD5 in Saos-2 cells was measured via western blot. (C) The proliferation of Saos-2 cells was assessed by CCK-8 assay. (D and E) The protein levels of OCN and RUNX2 in Saos-2 cells were examined by western blot. (F and G) The osteogenic differentiation of Saos-2 cells was analyzed by Alizarin Red staining. (H-G) After Saos-2 cells were transfected with si-NC, si-circ_KIAA0922, si-circ_KIAA0922 + anti-miR-NC, or si-circ_KIAA0922 + anti-miR-148a-3p, the mRNA and protein levels of SMAD5 were determined by qRT-PCR or western blot.

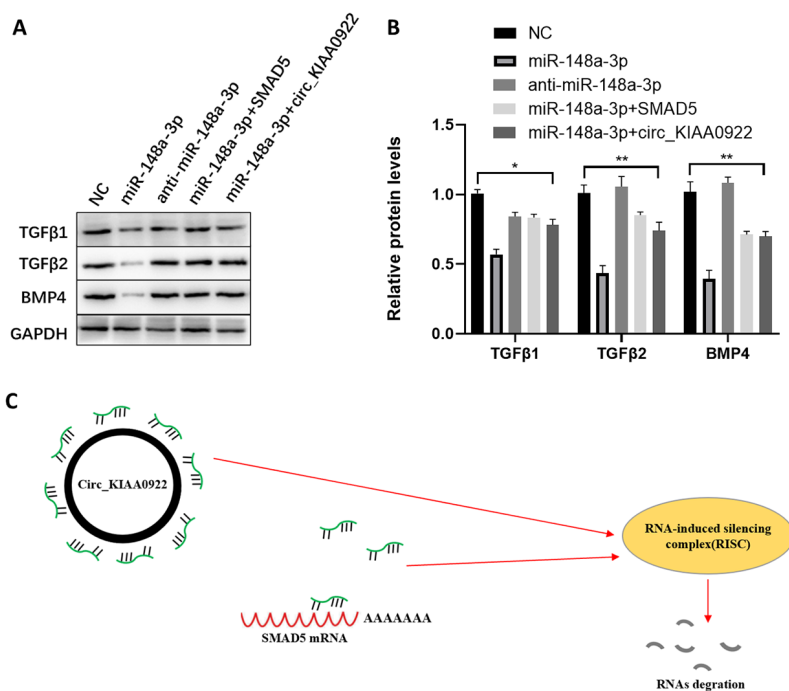


Figure 8. Circ_KIAA0922 targets miR-148a-3p/SMAD5 to regulate osteogenic differentiation and activate the TGF-β signaling pathway in Saos-2 cells. (A and B) The relative protein expression levels of TGF-β1, TGF-β2, and BMP4 were decreased in the miR-148a-3p group, increased in the anti-miR-148a-3p group, and rescued in the miR-148a-3p + SMAD5 and miR-148a-3p + circ_KIAA0922 groups. (C) The mechanistic diagram illustrates that the RNA-induced silencing complex (RISC) of miR-148a-3p, which degrades the SMAD5 mRNA, would be broken by circ_KIAA0922 binding to miR-148a-3p.

et al., 2020). Bone remodeling is a tightly controlled process in which osteoblasts (the cells responsible for bone formation), osteoclasts (the cells specialized for bone resorption), and osteocytes (the multifunctional mechanosensing cells embedded in the bone matrix) are the main actors. Increased oxidative stress in osteoblasts, the cells that produce and mineralize bone matrix, has been associated with the development of OP.

Saos-2 cells, also known as osteoblast-like cells, are derived from human osteosarcoma and have osteoblastic characteristics in that they can grow, differentiate, and cause mineralization of the extracellular matrix under certain induced conditions, which makes them an important cell line to study osteoblast differentiation (22). They are very easily induced to form a large number of mineralized nodules in a short period of time under the action of ascorbic acid and sodium B-glycerophosphate and are also able to express certain osteogenic mineralization signature genes and have a strong osteogenic capacity.

CircRNAs participate in a variety of physiological and pathological processes through diverse mechanisms, including miRNA sponging, interaction with proteins, and transformation into small peptides (23,24). It has been suggested that circRNAs may be used as diagnostic biomarkers or treatment targets in OP. For example, Wu *et al.* demonstrated that circRNA_003795 was able to promote the osteogenic differentiation activity of hBMSCs (25). Lin *et al.* claimed that the knockdown of circRNA IGSF11 increased miR-199b-5p expression and promoted osteoblast differentiation (26). According to Guan *et al.*, overexpression of circRNA_0021739 reduces miR-502-5p levels and inhibits osteoclasts differentiation (27). Circ-SLC8A1 is downregulated in OP and promotes OP development by miR-516b-5p/AKAP2 (28). These reports have indicated the involvement of circRNAs in OP. In this study, we demonstrated that circ_KIAA0922 was upregulated in Saos-2 cells during osteogenic differentiation. Moreover, circ_KIAA0922 knockdown inhibited the proliferation and osteogenic differentiation and reduced the osteogenic differentiation markers (OCN and RUNX2) in Saos-2 cells *in vitro*, indicating the positive regulatory role of circ_KIAA0922 in the osteogenic differentiation of Saos-2 cells. Thereafter, the downstream mechanism underlying the role of circ_KIAA0922 in the osteogenic differentiation of Saos-2 cells was further elucidated.

MicroRNAs are important regulatory factors necessary to maintain bone homeostasis, which is of great significance for bone health and diseases (29). Pan *et al.* demonstrated that miR-148a overexpression promoted osteoclastogenesis and bone resorption *in vitro* (30), and Liu *et al.* claimed that miR-148a-3p expression was restrained during osteoblast differentiation (21). Bedene *et al.* reported that the expression of miR-148a-3p was significantly higher in osteoporotic patients

(31). In line with these results, we found that miR-148a-3p inhibited osteogenic differentiation of Saos-2 cells *in vitro*. In addition, our findings revealed that circ_KIAA0922 inhibited the proliferation and osteogenic differentiation of Saos-2 cells by targeting miR-148a-3p.

SMAD5 is a critical downstream transcription factor for BMP2. Smad5 phosphorylation due to BMP2 signaling leads to a Smad5 complex formation, which translocates into the nucleus to transactivate the expression of osteogenic genes such as Runx2 and Atf4 (32). Previous studies have confirmed its essential role in skeletal development and bone formation (33). SMAD5 has been reported to enhance the expression of osteogenic markers, such as OCN and alkaline phosphatase (ALP) (33). The active TGF- β signaling pathway can negatively promote osteoblast maturation, mineralization, and osteoblast transformation (34). MiRNAs and their targets are mainly involved in the key signaling pathways that control bone formation, including the TGF- β /BMP/SMAD signaling pathways (5,35). However, previous studies have not confirmed the relationship between miR-148a-3p and SMAD5 in the process of osteogenic differentiation. In this study, we demonstrated that overexpression of SMAD5 promoted cell proliferation and osteogenic differentiation and increased OCN and RUNX2 levels in Saos-2 cells *in vitro*. Specifically, miR-148a-3p overexpression inhibited the osteogenic differentiation of Saos-2 cells *in vitro* by targeting SMAD5.

In summary, we showed that circ_KIAA0922 affected OP by regulating SMAD5/miR-148a-3p, providing the first line of evidence to clarify the underlying regulatory mechanisms of circ_KIAA0922 in the development of OP *in vitro*. Our findings provide a theoretical foundation for circ_KIAA0922 as a novel diagnostic biomarker and therapeutic target to improve osteogenic differentiation in OP. However, this was an *in vitro* study, and no *in vivo* experiments have been performed, which constitutes a limitation of the present study and calls for additional in-depth investigations in further studies.

Funding: This work was supported by a grant from the Natural Science Foundation of Shandong Province (General program ZR2023MH276) and Academic Promotion Program of Shandong First Medical University (LJ001).

Conflict of Interest: The authors have no conflicts of interest to disclose.

References

1. Tamma R, Zallone A. Osteoblast and osteoclast crosstalks: from OAF to Ephrin. *Inflamm Allergy Drug Targets*. 2012; 11:196-200.
2. Wang Z, Zhang H, Zhang P, Li J, Shan Z, Teng W. Upregulation of miR-2861 and miR-451 expression in papillary thyroid carcinoma with lymph node metastasis.

- Med Oncol. 2013; 30:577.
3. Zhang L, Zheng YL, Wang R, Wang XQ, Zhang H. Exercise for osteoporosis: A literature review of pathology and mechanism. *Front Immunol.* 2022; 13:1005665.
 4. Srivastava M, Deal C. Osteoporosis in elderly: prevention and treatment. *Clin Geriatr Med.* 2002; 18:529-555.
 5. Khosla S, Hofbauer LC. Osteoporosis treatment: recent developments and ongoing challenges. *Lancet Diabetes Endocrinol.* 2017; 5:898-907.
 6. Zhang Q, Wang W, Zhou Q, Chen C, Yuan W, Liu J, Li X, Sun Z. Roles of circRNAs in the tumour microenvironment. *Mol Cancer.* 2020; 19:14.
 7. Chen X, Ouyang Z, Shen Y, Liu B, Zhang Q, Wan L, Yin Z, Zhu W, Li S, Peng D. CircRNA_28313/miR-195a/CSF1 axis modulates osteoclast differentiation to affect OVX-induced bone absorption in mice. *RNA Biol.* 2019; 16:1249-1262.
 8. Huang W, Wu Y, Qiao M, Xie Z, Cen X, Huang X, Zhao Z. CircRNA-miRNA networks in regulating bone disease. *J Cell Physiol.* 2022; 237:1225-1244.
 9. Ye Y, Ke Y, Liu L, Xiao T, Yu J. CircRNA FAT1 Regulates Osteoblastic Differentiation of Periodontal Ligament Stem Cells via miR-4781-3p/SMAD5 Pathway. *Stem Cells Int.* 2021; 2021:5177488.
 10. Harper KL, McDonnell E, Whitehouse A. CircRNAs: From anonymity to novel regulators of gene expression in cancer (Review). *Int J Oncol.* 2019; 55:1183-1193.
 11. Yu L, Liu Y. circRNA_0016624 could sponge miR-98 to regulate BMP2 expression in postmenopausal osteoporosis. *Biochem Biophys Res Commun.* 2019; 516:546-550.
 12. Qiao L, Li CG, Liu D. CircRNA_0048211 protects postmenopausal osteoporosis through targeting miRNA-93-5p to regulate BMP2. *Eur Rev Med Pharmacol Sci.* 2020; 24:3459-3466.
 13. Yao X, Liu M, Jin F, Zhu Z. Comprehensive Analysis of Differentially Expressed Circular RNAs in Patients with Senile Osteoporotic Vertebral Compression Fracture. *Biomed Res Int.* 2020; 2020:4951251.
 14. Ji H, Cui X, Yang Y, Zhou X. CircRNA hsa_circ_0006215 promotes osteogenic differentiation of BMSCs and enhances osteogenesis-angiogenesis coupling by competitively binding to miR-942-5p and regulating RUNX2 and VEGF. *Aging (Albany NY).* 2021; 13:10275-10288.
 15. Bao H, Zhou Q, Li Q, Niu M, Chen S, Yang P, Liu Z, Xia L. Differentially expressed circular RNAs in a murine asthma model. *Mol Med Rep.* 2020; 22:5412-5422.
 16. Xie Y, Cao Y, Guo CJ, Guo XY, He YF, Xu QY, Shen F, Pan Q. Profile analysis and functional modeling identify circular RNAs in nonalcoholic fatty liver disease as regulators of hepatic lipid metabolism. *Front Genet.* 2022; 13:884037.
 17. Wang X, Ning Y, Yang L, Liu H, Wu C, Wang S, Guo X. Diagnostic value of circulating microRNAs for osteosarcoma in Asian populations: a meta-analysis. *Clin Exp Med.* 2017; 17:175-183.
 18. Mi B, Xiong Y, Chen L, Yan C, Endo Y, Liu Y, Liu J, Hu L, Hu Y, Sun Y, Cao F, Zhou W, Liu G. CircRNA AFF4 promotes osteoblast cells proliferation and inhibits apoptosis via the Mir-7223-5p/PIK3R1 axis. *Aging (Albany NY).* 2019; 11:11988-12001.
 19. Du YX, Guo LX, Pan HS, Liang YM, Li X. Circ_ANKIB1 stabilizes the regulation of miR-19b on SOCS3/STAT3 pathway to promote osteosarcoma cell growth and invasion. *Hum Cell.* 2020; 33:252-260.
 20. Mizoguchi F, Murakami Y, Saito T, Miyasaka N, Kohsaka H. miR-31 controls osteoclast formation and bone resorption by targeting RhoA. *Arthritis Res Ther.* 2013; 15:R102.
 21. Liu N, Sun Y. microRNA-148a-3p-targeting p300 protects against osteoblast differentiation and osteoporotic bone reconstruction. *Regen Med.* 2021; 16:435-449.
 22. Prideaux M, Wijenayaka AR, Kumarasinghe DD, Ormsby RT, Evdokiou A, Findlay DM, Atkins GJ. SaOS2 Osteosarcoma cells as an *in vitro* model for studying the transition of human osteoblasts to osteocytes. *Calcif Tissue Int.* 2014; 95:183-193.
 23. He T, Liu W, Cao L, Liu Y, Zou Z, Zhong Y, Wang H, Mo Y, Peng S, Shuai C. CircRNAs and LncRNAs in Osteoporosis. *Differentiation.* 2020; 116:16-25.
 24. Sun Z, Chen C, Su Y, Wang W, Yang S, Zhou Q, Wang G, Li Z, Song J, Zhang Z, Yuan W, Liu J. Regulatory mechanisms and clinical perspectives of circRNA in digestive system neoplasms. *J Cancer.* 2019; 10:2885-2891.
 25. Wu J, Ren W, Zheng Z, Huang Z, Liang T, Li F, Shi Z, Jiang Q, Yang X, Guo L. Mmu_circ_003795 regulates osteoblast differentiation and mineralization in MC3T3-E1 and MDPC23 by targeting COL15A1. *Mol Med Rep.* 2020; 22:1737-1746.
 26. Zhang M, Jia L, Zheng Y. circRNA Expression Profiles in Human Bone Marrow Stem Cells Undergoing Osteoblast Differentiation. *Stem Cell Rev Rep.* 2019; 15:126-138.
 27. Guan J, Gan L, Jin D, Wu X, Cheng L, Liu M, Fan Y, Zhou J, Zhang H, Zhang Y, Zhou P. Overexpression of circ_0021739 in Peripheral Blood Mononuclear Cells in Women with Postmenopausal Osteoporosis Is Associated with Reduced Expression of microRNA-194-5p in Osteoclasts. *Med Sci Monit.* 2021; 27:e929170.
 28. Lin C, Zhong W, Yan W, Yang J, Zheng W, Wu Q. Circ-SLC8A1 regulates osteoporosis through blocking the inhibitory effect of miR-516b-5p on AKAP2 expression. *J Gene Med.* 2020; 22:e3263.
 29. Grillari J, Mäkitie RE, Kocijan R, Haschka J, Vázquez DC, Semmelrock E, Hackl M. Circulating miRNAs in bone health and disease. *Bone.* 2021; 145:115787.
 30. Pan B, Zheng L, Liu S, Fang J, Lou C, Hu X, Ye L, Lai H, Gao J, Zhang Y, Ni K, He D. MiR-148a deletion protects from bone loss in physiological and estrogen-deficient mice by targeting NRP1. *Cell Death Discov.* 2022; 8:470.
 31. Bedene A, Mencej Bedrač S, Ješe L, Marc J, Vrtačnik P, Prezelj J, Kocjan T, Kranjc T, Ostanek B. MiR-148a the epigenetic regulator of bone homeostasis is increased in plasma of osteoporotic postmenopausal women. *Wien Klin Wochenschr.* 2016; 128:519-526.
 32. Ellur G, Sukhdeo SV, Khan MT, Sharan K. Maternal high protein-diet programs impairment of offspring's bone mass through miR-24-1-5p mediated targeting of SMAD5 in osteoblasts. *Cell Mol Life Sci.* 2021; 78:1729-1744.
 33. Nishimura R, Kato Y, Chen D, Harris SE, Mundy GR, Yoneda T. Smad5 and DPC4 are key molecules in mediating BMP-2-induced osteoblastic differentiation of the pluripotent mesenchymal precursor cell line C2C12. *J Biol Chem.* 1998; 273:1872-1879.
 34. Wu M, Chen G, Li YP. TGF- β and BMP signaling in osteoblast, skeletal development, and bone formation, homeostasis and disease. *Bone Res.* 2016; 4:16009.
 35. Iaquinta MR, Lanzillotti C, Mazziotta C, Bononi I,

Frontini F, Mazzoni E, Oton-Gonzalez L, Rotondo JC, Torreggiani E, Tognon M, Martini F. The role of microRNAs in the osteogenic and chondrogenic differentiation of mesenchymal stem cells and bone pathologies. *Theranostics*. 2021; 11:6573-6591.

Received August 30, 2023; Revised October 24, 2023;
Accepted October 31, 2023.

**Address correspondence to:*

Yanqin Lu and Jinxiang Han, Shandong First Medical University & Shandong Academy of Medical Sciences, # 6699 Qingdao Road, Ji'nan, Shandong 250117, China.
E-mail: yqlu@sdfmu.edu.cn (YL), jxhan@sdfmu.edu.cn (JH)

Released online in J-STAGE as advance publication November 2, 2023.